JPET Fast Forward. Published on September 16, 2015 as DOI: 10.1124/jpet.115.225912
This article has not been copyedited and formatted. The final version may differ from this version.

LG308, a novel synthetic compound with anti-microtubule activity in prostate cancer cells, exerts effective antitumor activity

Min Qin, Shihong Peng, Ning Liu, Meichun Hu, Yundong He, Guoliang Li, Huang Chen, Yuan He, Ang Chen, Xin Wang, Mingyao Liu, Yihua Chen and Zhengfang Yi

Shanghai Key Laboratory of Regulatory Biology, Institute of Biomedical Sciences and School of Life Sciences, East China Normal University, Shanghai, China (M.Q., S.P., N.L., M.H., Y.H., G.L., H.C., Y.H., A.C., X.W., M.L., Y.C., Z.Y.); Center for Cancer and Stem Cell Biology, Institute of Biosciences and Technology and Department of Molecular and Cellular Medicine, Texas A&M University Health Science Center, Houston, Texas, United States of America (M.L.)

JPET Fast Forward. Published on September 16, 2015 as DOI: 10.1124/jpet.115.225912
This article has not been copyedited and formatted. The final version may differ from this version.

LG308 suppresses PCa by blocking microtubule polymerization

Zhengfang Yi, Shanghai Key Laboratory of Regulatory Biology, Institute of Biomedical Sciences and School of Life Sciences, East China Normal University, 500 Dongchuan Rd, Shanghai, 200241, China, +86-21-54345016(Phone and Fax), zfyi@bio.ecnu.edu.cn (Email)
Yihua Chen, Shanghai Key Laboratory of Regulatory Biology, Institute of Biomedical Sciences and School of Life Sciences, East China Normal University, 500 Dongchuan Rd, Shanghai, 200241, China, +86-21-24206647(Phone),+86-21-54344922(Fax), yhchen@bio.ecnu.edu.cn (Email)

Number of text pages: 37;
Number of tables: 0;
Number of figures: 5;
Number of references: 39;
Number of words in the Abstract: 214;
Number of words in the Introduction: 514;
Number of words in the Discussion: 808.

List of nonstandard abbreviations

ATCC, American Type Culture Collection; BSA, bull serum albumin; CRPC, castration-resistant prostate cancer; DAPI, 4', 6-diamidino-2-phenylindole; DMSO, dimethyl sulfoxide; EDTA, ethylenediaminetetraacetic acid; EGTA, ethylene glycol tetraacetic acid; IC_{50}, half maximal inhibitory concentration; IHC, immunohistochemistry; PAGE, SDS-polyacrylamide gel electrophoresis; PBS, phosphate buffered saline; PCa, prostate cancer; PI, propidium iodide; PMSF, phenylmethylsulfonyl fluoride; RNAase, ribonuclease ; SDS, sodium sodecyl sulfate; SRB, sulforhodamine B.

Recommended Section

Drug Discovery and Translational Medicine

Abstract

Microtubule plays many different essential roles in the process of tumorigenesis in many eukaryotes, and targeting mitotic progression by disturbing microtubule dynamics is utilized as a common strategy for cancer treatment. Microtubule-targeted drugs, including paclitaxel and *Vinca* alkaloids, were previously considered to work primarily by increasing or decreasing the cellular microtubule mass. The tubulin/microtubule system, which is an integral component of the cytoskeleton, is a therapeutic target for prostate cancer. Herein, we found a novel synthetic compound 8-fluoro-*N*-phenylacetyl-1, 3, 4, 9-tetrahydro-β-carboline (LG308), which disrupted the microtubule organization via inhibiting the polymerization of microtubule in PC-3M and LNCaP prostate cancer cell lines. Further study proved that LG308 induced the mitotic phase arrest and inhibited G2/M progression significantly in LNCaP and PC-3M cell lines in a dose-dependent manner, which were associated with the upregulation of cyclin B1 and mitotic marker MPM-2 and the dephosphorylation of cdc2. Besides, the cell proliferation and colony formation of PC-3M and LNCaP cells were effectively inhibited by LG308. Furthermore, LG308 induced apoptosis and cell death in PC-3M and LNCaP cell lines *in vitro*. *In vivo*, LG308 dramatically suppressed the growth and metastasis of prostate cancer in both xenograft and orthotopic models. All these data indicate that LG308 is a promising anticancer candidate with antimitotic activity for the treatment of prostate cancer.

JPET Fast Forward. Published on September 16, 2015 as DOI: 10.1124/jpet.115.225912
This article has not been copyedited and formatted. The final version may differ from this version.

Introduction

In all eukaryotic cells, microtubule, as one of the main components of the cell cytoskeleton, plays many different essential roles including the maintenance of cell shape, intracellular transport, cell motility, meiosis, and mitosis (Amos, 2000; Jordan and Wilson, 2004). Previous studies showed that microtubule dynamics was crucial for cell function (Wilson and Jordan, 1995). In addition, microtubule is extremely important in the process of mitosis in orchestrating the separation and segregation of chromosomes, which sheds lights that microtubule is an important target for the research and development of anticancer drugs (Risinger et al., 2009a; Stumpff et al., 2014). All microtubule-targeted drugs can disrupt the dynamics of microtubule and induce mitosis arrest of tumor cells (McIntosh and Hering, 1991). Anti-mitotic drugs can be classified into two groups, one inhibits microtubule polymerization, such as colchicine and vinorelbine, while the other stimulates microtubule depolymerization, such as paclitaxel and docetaxel (Desbene and Giorgi-Renault, 2002).

Prostate cancer (PCa) is a kind of common malignant tumor in male genitourinary system. Among men, PCa is the most frequently diagnosed new cases of cancer and the second leading cause of cancer death in the United States (Siegel et al., 2015). With the development of society and the improvement of people's living standards, as well as the changed dietary structure along with the aging tendency of population and hormone misuse, it can be doubtlessly estimated that the incidence of PCa in the whole world will increase rapidly, which attracts even much more attention (Ren et al., 2013). At

JPET Fast Forward. Published on September 16, 2015 as DOI: 10.1124/jpet.115.225912
This article has not been copyedited and formatted. The final version may differ from this version.

present, surgical treatment, radiation treatment, hormone treatment and chemical therapy are four most common therapeutic methods for PCa patients. Hormone treatment, which is also termed as androgen-deprivation therapy, is the critical therapeutic option for advanced PCa patients among the above four therapies (Jani and Hellman, 2003; Ponholzer et al., 2011). Unfortunately, hormonal therapy just has a palliative benefit in the early stage of PCa treatment and the majority of patients eventually progress to androgen-independent or hormone-refractory PCa, which means androgen-deprivation therapy is no longer effective and the cancer continues to develop (Miyamoto et al., 2004). Therefore, chemotherapy of the advanced hormone-refractory PCa draws much more attention over the last few decades. Some microtubule-targeted agents have been demonstrated overall survival benefit clinically (Suzman and Antonarakis, 2014). Nowadays, some chemo-drugs targeting at microtubule and tubulin including docetaxel, cabazitaxel, epothilones and vinorelbine have been clinically used as chemotherapy drugs for androgen-independent PCa (Caty et al., 1997; Kearns et al., 2013; Morganti et al., 2013). Nevertheless, drug resistance often appears after prolonged treatment. Therefore, researching and developing some novel anti-microtubule candidates is a potential strategy for hormone-refractory PCa (Aneja et al., 2010).

In this study, a novel compound with tetrahydro-β-carboline scaffold, named LG308 (Fig. 1A，MW: 308.3495), was synthesized, screened and identified as an anticancer agent in our laboratory. Our results indicated that LG308 induced G2/M cell cycle arrest through inhibiting microtubule polymerization and disrupting the microtubule

JPET Fast Forward. Published on September 16, 2015 as DOI: 10.1124/jpet.115.225912
This article has not been copyedited and formatted. The final version may differ from this version.

assembly. Further study suggested that LG308 inhibited the proliferation of PCa cells and induced cell apoptosis and cell death. More importantly, LG308 suppressed xenograft and orthotopic PC-3M tumor growth and metastasis.

JPET Fast Forward. Published on September 16, 2015 as DOI: 10.1124/jpet.115.225912
This article has not been copyedited and formatted. The final version may differ from this version.

Materials and methods

Synthesis of LG308

To a solution of 2-fluorophenylhydrazine hydrochloride (0.81 g, 5.00 mM) in 30 mL of EtOH/H_2O (v/v = 5/1) was added 4-chloro-1, 1-dimethoxybutane (0.84 g, 5.50 mM) and heated to reflux for 2 h. Then the solvent was removed under vacuum and the residue was chromatographed through silica gel eluding with CH_2Cl_2/MeOH (30:1) to give the 7-fluorotryptamine (0.37 g) as an oil. Subsequently aq. HCHO (1.56 mL) was added to the solution of 7-fluorotryptamine (0.37 g, 2.08 mM) in CH_3COOH (15 mL) with drop-wised manner. The mixture was stirred at room temperature for 12 h at the atmosphere of N_2, then the solvent was removed under vacuum and the residue was chromatographed through silica gel eluding with CH_2Cl_2/MeOH (40:1) to afford the 8-fluoro-1, 3, 4, 9-tetrahydro-β-carboline (0.36 g) as a white powder. At last, to a solution of phenylacetic acid (283 mg, 2.08 mM) in anhydrous DMF (3 mL) were added EDC·HCl (518 mg, 2.70 mM) and HOBt (309 mg, 2.29 mM) at 0 ^{o}C, and then 8-fluoro-1,3,4,9-tetrahydro-β-carboline (0.36 g, 1.89 mM) was added to the mixture after stirring for 15 min. The mixture was stirred for another 3 h, diluted with H_2O, and extracted with EtOAc. The combined organic phase was dried over anhydrous Na_2SO_4, concentrated, and chromatographed over silica gel to give 0.54 g of 8-fluoro-*N*-phenylacetyl-1, 3, 4, 9-tetrahydro-β-carboline (LG308). The synthesis route of LG308 is described in Supplemental Figure 1A .

JPET Fast Forward. Published on September 16, 2015 as DOI: 10.1124/jpet.115.225912
This article has not been copyedited and formatted. The final version may differ from this version.

Cell Lines, animals and reagents

Human PCa cell lines PC-3M, DU145, 22RV1 and PC3 were purchased from ATCC. Human normal prostate epithelium immortalized cell line PNT1A and human PCa cell line LNCaP were kind gifts from Professor Hanyi Zhuang of Shanghai Jiaotong University. PC-3M cells were cultured in Dulbecco's Modified Eagle Medium (Gibco). LNCaP, PNT1A, PC3, DU145 and 22RV1 cells were maintained in RPMI-1640 medium (Gibco). Both mediums were supplemented with 10% fetal bovine serum (Wisent). In addition, PC-3M cells were transfected with pGL4 vector (Promega) and selected in G418 for stable PC-3M-luc cell line. All cells were incubated at 37 ^{o}C with 5% humidified CO_2. Mice were obtained from National Rodent Laboratory Animal Resources, Shanghai Branch of China. All animal experimental protocols were approved by the Animal Investigation Committee of the Institute of Biomedical Sciences, East China Normal University. The antibodies used in this study were anti-cdc 2, p-cdc 2, cdc 25c, cyclin B1, Caspase 3, PARP, β-actin (Cell Signaling Technology), α-tubulin (Epitomics), CD31 (Abcam) and anti-phospho-Ser/Thr-Pro MPM-2 (Millipore). The compound LG308 was synthesized by our lab with the purity more than 98%.

Cell proliferation assay (Sulforhodamine B assay)

Cell proliferation inhibition assay was determined by Sulforhodamine B assay. Briefly, 4000 cells per well were seeded in 96-well plates. After 24 h, cells were exposed to five different dose (0, 1, 5, 10, 20 μM) of LG308 for 72 h. Cells were fixed

JPET Fast Forward. Published on September 16, 2015 as DOI: 10.1124/jpet.115.225912
This article has not been copyedited and formatted. The final version may differ from this version.

with 10% trichloroacetic acid for 1 h at 4 ^{o}C, washed five times with flowing water, and then air-dried. Cells were stained with 50 μL 0.4% (w/v) SRB for 20 min at room temperature, washed five times with 1% acetic acid, and then air-dried. 100 μL 10 mM Tris was added per well, and absorbance was measured at 515 nm.

Colony formation assay

Cells were splitted with trypsin and seeded 2000 (PC-3M, PC3, DU145) or 4000 (LNCaP, 22RV1) per well in 6-well dishes. Cells were allowed to attach overnight and then exposed to different doses of LG308 for a week. After fixed with 4% paraformaldehyde for 20 min in room temperature, cells were stained with 0.2% crystal violet. The number of cell colonies was calculated and analyzed as the ratio of the number of treated samples to untreated samples. Triplicate wells were set up for each dose.

Cell cycle distribution analysis

Cells were initially seeded in 6cm dishes. After incubation for 24 h, cells were treated with four different dose (0, 5, 10, 20 μM) of LG308 for 24 h. After washed with PBS and digested with trypsin, adherent and floating cells were collected, washed once with PBS, and then fixed in cold 70% ethanol overnight in 4 ^{o}C. After ethanol fixation, cells were washed in PBS once and suspended in PBS with 200 μg/mL RNAase and 50 μg/mL propidium iodide (PI) in the dark for 30 min. Then cells were analyzed by flow cytometry (FACS Calibur; BD Biosciences).

JPET Fast Forward. Published on September 16, 2015 as DOI: 10.1124/jpet.115.225912
This article has not been copyedited and formatted. The final version may differ from this version.

Immunofluorescence staining

Immunofluorescence staining was performed according to previous report (Zhang et al., 2011). Briefly, cells were seeded on gelatin-coated-glass cover slips. 24 h later, cells were treated with different dose of LG308 for 24 h. Then cells were incubated with 4% paraformaldehyde for 20 min, washed with PBS, and treated with 0.5% Triton-X 100, washed with PBS. After blocking in 0.5% BSA, cells were incubated with primary antibody overnight at 4 ^{o}C before further incubation with secondary antibody at 37℃ for 1 h in the dark. Then DAPI was added for 5 min in the dark. Images were recorded by confocal microscopy (Leica).

Mitotic index assay

Mitotic index assay was performed according to previous report (Chang et al., 2011) with modification. Cells were seeded on gelatin-coated cover slips. After 24 h, four different doses (0, 5, 10, 20 μM) compound were added for 24 h. After fixed with 4% paraformaldehyde for 20 min at room temperature, cells were permeabilized with 0.2% Triton-X 100 in PBS for 5 min. The nuclei were stained with DAPI. After washed with PBS, cells were visualized and photographed with Leica microscopy. Five random fields were counted and analyzed. Mitotic index was calculated by dividing the total number of examined cells by the number of cells in mitosis.

Western blotting

Cells were exposed to five different dose (0, 1, 5, 10, 20 μM) of LG308 for indicated time and lysed in RIPA buffer [50 mM Tris–HCl (pH 7.4), 150 mM NaCl, 5 mM EDTA,

JPET Fast Forward. Published on September 16, 2015 as DOI: 10.1124/jpet.115.225912
This article has not been copyedited and formatted. The final version may differ from this version.

1 % Triton X-100, 1 % sodium deoxycholic acid, 0.1% SDS, 2 mM phenylmethylsulfonyl fluoride (PMSF), 30 mM Na_2HPO_4, 50 mM NaF, 1 mM Na_3VO_4] containing protease/phosphatase inhibitors (Roche). Lysates were mixed with sample loading buffer and heated at 100 ^oC for 10 min. After separated by SDS-polyacrylamide gel electrophoresis (PAGE), extracted protein were transferred to nitrocellulose membranes. Membranes were blocked with 5% skim milk in PBS and 0.1% Tween-20 and then incubated with specific primary antibodies over night at 4 ^oC. Then membranes were exposed to secondary antibodies for 2 h at room temperature. Immunoreactive proteins were visualized using the Odyssey Fluorescence Scanner (LI-COR Bioscience, Inc., Lincoln, NE, USA).

Apoptosis analysis

Apoptosis analysis was carried out by flow cytometry (FACS Calibur; BD Biosciences). Cells were treated with four different doses (0, 5, 10, 20 μM) of LG308 for 48 h or with 10 μM LG308 for different time. Cells were washed with PBS, then harvested by 0.25% trypsin and washed with PBS again, followed by resuspending in binding buffer. After that, 5μL Annexin V fluorescein isothiocyanate and 5 μL propidium iodide were added and the mixture was kept in the dark for 15 min at room temperature, then 400 μL of binding buffer was added and analyzed immediately with flow cytometry (FACS Calibur; BD Biosciences).

Viability assay

Viability assay was performed using the live/dead viability/cytotoxicity kit

JPET Fast Forward. Published on September 16, 2015 as DOI: 10.1124/jpet.115.225912
This article has not been copyedited and formatted. The final version may differ from this version.

(Molecular Probes). This kit contains calcein-AM to stain the living cells (green) and ethidium homodimer-1 (EthD-1) to stain the dead cells (red). Briefly, cells were exposed to five different doses (0, 1, 5, 10, 20 μM) of LG308 for 48 h, then 2 μM calcein AM and 4 μM EthD-1 working solution was added. After incubated at room temperature for 30 min, the green living and the red dead cells were visualized by Fluorescence microscopy and photographed. Cells from three random areas per sample were counted for statistical analysis.

In vivo microtubule polymerization assay

In vivo microtubule polymerization assay was performed according to previous reports (Aneja et al.; Chang et al.; Shi et al.; Zhao et al.; Kuo et al., 2004) with modification. PC-3M and LNCaP cells were seeded on 6-well plates. After 24 h, cells were exposed to four different doses (0, 5, 10, 20 μM) of LG308, 50 nM colchicine and 50 nM paclitaxel for 24 h, respectively. Cells then were washed with PBS for three times before adding lysis buffer containing 20 mM Tris-HCL (PH6.8), 1 mM $MgCl_2$, 2 mM EGTA and Protease inhibitor and phosphatase inhibitor and 0.5% nonidet. Supernatants were collected after centrifugation at 14000 rpm for 10 min. Supernatants and the pellets were dissolved in SDS-PAGE sampling loading buffer at 95 ^{o}C for 10 min. Supernatants containing soluble tubulin and the pellets (the polymerized tubulin lysates) were subjected to 10% SDS-PAGE before Western blotting.

Xenograft model of human prostate cancer PC-3M tumor

PC-3M cells (2×10^6) were implanted subcutaneously on the right side of the dorsal area of 4-week-old male nude mice. 10 days later, mice were divided into two groups (n = 8) randomly. Using the appropriate dose according the preliminary test, LG308 (25 mg/kg) was injected intraperitoneally every day. Control group was treated with dimethyl sulfoxide (DMSO). 20 days later, mice were sacrificed, tumors were removed and images were taken. The growth rate of the tumor xenograft was evaluated by determining the tumor volume using digital caliper every day. Tumor growth rate was measured as the following equation, volume=length × width^2 × 0.52. Mice were continually observed until they were sacrificed (Dong et al., 2010).

PC-3M orthotopic tumor growth and metastasis

Male nude mice were anesthetized and placed under a sterile cover in a supine position. An incision was made 3 mm above the pubic symphysis and the bladder and seminal vesicles were carefully lifted to expose the dorsal prostate. The PC-3M-luc cells suspension (1×10^6 cells in 0.05 mL PBS) was injected into the dorsal prostate (Zhang et al.; Pettaway et al., 1996; Tuomela et al., 2008). After inoculation, abdominal muscle layer and the skin were closed and sewed up, respectively. One week later, the mice were then segregated into 3 groups (n = 8) based on Xenogen IVIS 2000 Luminal Imager (IVIS imaging system 100, Xenogen Corporation). All mice were intraperitoneally injected with LG308 (10 mg/kg and 25 mg/kg) every day, with an equivalent volume of DMSO injected in control animals. And the mice were treated

JPET Fast Forward. Published on September 16, 2015 as DOI: 10.1124/jpet.115.225912
This article has not been copyedited and formatted. The final version may differ from this version.

consecutively for 20 days, with the measurement of body weight and IVIS image.

Hematoxylin and eosin (HE) and immunohistochemistry (IHC)

HE staining and immunohistochemistry were performed as reported previously (Zhang et al., 2012). Tumors, liver and kidney were removed from sacrificed mice, fixed with 10% formaldehyde and then embedded in paraffin. Paraffinembedded tissues were sectioned at 5μm Sections. Tumor tissues were stained with MPM-2 (Millipore) and CD31 (Abcam). The HE staining of liver and kidney was performed according to standard protocol. Images were taken with Leica microscope. The results were analyzed using Image-Pro Plus 6.0 software.

Determination of LG308 in nude mouse plasma

Blood was sampled from mouse eyes at 10min, 30min, 1h, 2h, 4h, and 8h after intraperitoneal administration. The concentration of LG308 in plasma was determined by an Agilent 1290 LC system coupled with 6460 triple-quadrupole mass spectrometer (Agilent Technologies, USA). Chromatography separation was performed on a Phenomenex Kinetex XB-C18 column (3.0 × 100 mm, 2.6 μm). The mobile phase consisted of water (A) and acetonitrile (B) using gradient elution at a flow rate of 0.3 mL/min, and the injection volume was 4 μL. The detection of the ions was performed in the MRM mode, monitoring the transition of m/z 307.2 precursor to the m/z 159.9 product ion for LG308, and m/z 401.3 precursor to m/z 254 product ion for IS (an analogue of compound). The fragmentor and collision energy were optimized for LG308 and IS, respectively. A liquid-liquid extraction method by ethyl acetate was used to isolate LG308 from plasma.

Statistical analysis

Dose- and time-dependent effects were analyzed using one-way ANOVA. The analysis of tumor volume and body weight varies with time in animal model were employed by Wald test. Other parameters were defined with an unpaired student's t-test; P value <0.05 was considered significant. P values for all experiments analyzed were indicated.

JPET Fast Forward. Published on September 16, 2015 as DOI: 10.1124/jpet.115.225912
This article has not been copyedited and formatted. The final version may differ from this version.

Results

LG308 inhibits proliferation and colony formation of PCa cells

Firstly the anti-proliferative effect of LG308 against normal prostate or PCa cells was determined by Sulforhodamine B assay, as indicated in PC-3M, LNCaP, PC3, DU145 and 22RV1 cell lines (PCa cell line) and PNT1A cell line (a human normal prostate epithelium immortalized cell line). In these assays, LG308 inhibited the proliferation of PC-3M, LNCaP, PC3, DU145 and 22RV1 cells, while it just showed slight effect on the PNT1A cell (Fig. 1B). For example, after the treatment of LG308, the half maximal inhibitory concentrations (IC_{50}) were shown about 5 μM against LNCaP and PC-3M PCa cell lines, compare to about 90% viability of normal prostatic cell PNT1A at the same concentration. When treated with 20 μM of LG308, the viability of LNCaP and PC-3M cells was dramatically deceased to 30% whereas just nearly 20% decrease for PNT1A cells, which indicated that LG308 showed more potent cytotoxic effect on PCa cells than on normal prostate epithelium cells. In addition, the colony formation assay was performed for illustrating the ability of cell proliferation more specifically. In accordance with SRB assay, LG308 inhibited colony formation in dose-dependent manner, and the most significant difference in colony formation between LG308 treated cells and control cells was shown at 5 μM LG308 (Fig. 1C and Supplemental Figure 1B). All these results demonstrated that LG308 inhibited the proliferation of PCa cells and possessed great selectivity between prostate normal cells and PCa cells.

JPET Fast Forward. Published on September 16, 2015 as DOI: 10.1124/jpet.115.225912
This article has not been copyedited and formatted. The final version may differ from this version.

LG308 induces cell cycle arrest of LNCaP and PC-3M cell lines

To verify the causal relation of the inhibitory cell proliferation and cell cycle arrest of LNCaP and PC-3M cells after treated with LG308, the cell cycle distribution was analyzed by flow cytometry. LG308 was found to increase cell number at G2/M phase after 24 h treatment with raising concentration, accompanied by decreased cell number at S phase and G1 phase in LNCaP and PC-3M cell lines (Fig. 1D) and similar cell cycle arrest effect was also detected in PNT1A cells (Supplemental Figure 1C). Furthermore, proteins responsible for G2/M transition were measured by western blotting. As expected, the rational results were consistent with the cell cycle assay. LG308 caused dose-dependent decreases in phosphorylated cdc2 and total cdc25c and an accumulation of cyclin B1 in PC -3M and LNCaP after 24h treatment (Fig. 1E). Meanwhile, the level of total cdc2 was not affected by the treatment of LG308 (Fig. 1E). Conclusively, these results indicated that LG308-induced cell cycles were arrested in G2/M phase before cell death occurred.

LG308 arrests cell cycle in mitotic phase

Next, the mitosis index assay was performed referred to the published report by staining the cells with DAPI to confirm whether cells were arrested at G2 or M phase (Chang et al., 2011). As shown in Figure 2A, with an increasing dose of LG308, more cells were accumulated at M phase as indicated by condensed nuclei in PC-3M, and LNCaP showed the similar M phase cells accumulation responding to LG308 treatment (Supplemental Figure 2A). Furthermore, we conducted the western blotting assay to

JPET Fast Forward. Published on September 16, 2015 as DOI: 10.1124/jpet.115.225912
This article has not been copyedited and formatted. The final version may differ from this version.

detect the MPM-2, a marker for mitotic cells. As Figure 2B shown, MPM-2 was up-regulated accompanied by the increase of LG308 concentration. The up-regulation of MPM-2 were also observed in LNCaP cells (Supplemental Figure 2B).

LG308 disrupts microtubule organization of PC-3M and LNCaP cells

Microtubules are composed of α-tubulin and β-tubulin heterodimers and plays critical roles in regulating cell cycle and cell proliferation(Jordan and Wilson, 2004). Conventionally, α-tubulin and β-tubulin heterodimers exist in two forms, soluble monomer and polymerized tubulin heterodimers. Our results showed that inhibitory effects of LG308 on PCa cell growth was related to cell mitosis arrest, which might be regulated by microtubular dynamics. The *in vivo* microtubule polymerization assay was performed on PC-3M and LNCaP cells to investigate the effect of LG308 on microtubule polymerization. After soluble and polymerized tubulin extracted, we discovered that polymerized tubulin decreased in a dose-dependent manner in response to LG308 treatment with a peak shown at dose 10mM (Fig. 2C). It was then examined how LG308 affected microtubule by immunofluoresce staining of the microtubule. We found most of cells were affected (data not shown). Furthermore, as shown in Figure 2D, cells exposed to LG308 presented disorganized microtubule distribution and more diffuse staining occurred throughout the cytoplasm with LG308 increased, which was similar to those of colchicine-induced microtubule change. In contrast, 50 nM of paclitaxel dramatically promoted microtubule polymerization with an increase in the density of cellular microtubules and formation of long thick microtubule bundles. Furthermore, as showed in Figure 2E, cells without treatment of LG308 presented

JPET Fast Forward. Published on September 16, 2015 as DOI: 10.1124/jpet.115.225912
This article has not been copyedited and formatted. The final version may differ from this version.

intact spindle assembly, while spindle structure was disrupted and showed an irregular organization with scattered stain increased after treatment of LG308. This phenomenon was also similar to that of spindle structure changed after the induction of colchicine treatment, with a reverse phenomenon caused by paclitaxel. The same results were also observed in LNCaP cells (Supplemental Figure 3A and 3B).

LG308 provokes PCa cell apoptosis as well as cell death

Besides the anti-microtubule activity, the effects of LG308 were further explored on apoptosis and cell death of PCa cells. To further identify whether LG308 could induce apoptosis in PCa cells, apoptosis analysis was investigated by staining PC-3M cells with Annexin V-FITC/PI. Results showed that LG308 induced apoptosis of PC-3M in both concentration-dependent and time-dependent manners. As shown in Fig. 3A and 3B, apoptotic cells raised from 1.79% to 11.39% with LG308 dose increased from 0 μM to 20 μM after 48 h treatment and raised from 2.23% to 17.94% along with treatment time increased from 0 h to 72 h at 10 μM. Then some downstream apoptotic proteins, such as caspse-3 and PARP were detected. Caspse-3 was down-regulated in a dose-dependent manner at 48 h and PARP was down-regulated by the increase of LG308 concentration at 72 h in PC-3M cells (Supplemental Figure 2C). Meanwhile, a cell viability assay was also carried out on PC-3M and LNCaP cells using the live/dead viability/cytotoxicity kit (Molecular Probes) to investigate whether LG308 resulted in the death of PCa cells. As revealed in Figure 3C, the percentage of dead cells ascended with the increase of LG308 concentration. These data indicated that LG308 also provoked apoptosis and cell death in addition to its effect on cell cycle.

JPET Fast Forward. Published on September 16, 2015 as DOI: 10.1124/jpet.115.225912
This article has not been copyedited and formatted. The final version may differ from this version.

LG308 inhibits the growth of PC-3M tumor xenograft

Above data suggested that LG308 inhibit PCa cell *in vitro*. Naturally, the effects of LG308 (25mg/kg/d) on PC-3M tumor xenograft was tested to investigate the effect of LG308 on PCa *in vivo*. As shown in Figure 4A, LG308 inhibited the growth of PC-3M tumor compared to the control group. The average tumor size of control group was 2510.62 ± 800.91 mm^3, whereas tumor size in LG308-treated group was 1190.85 ± 296.91 mm^3. The average tumor weight of the control group was 332.78 ± 101.9mg, while the LG308-treated group was 178.16 ± 52.86 mg. At the same time, treatment of LG308 at the given concentration had little effect on the body weights of the LG308-treated mice (Fig. 4A), and the HE staining results of liver and kidney confirmed the same conclusion that LG308 presented no obvious influence to the anatomical morphologies of mice administrated with LG308 (Fig. 4C), when compared to the control group. These data may suggested that LG308 had low toxicity to mouse at the curative dose. At the same time, less cell proliferation as indicated by probes anti-Ki-67 and accumulation of M phase cells as indicated by probes anti-MPM2 (Fig. 4B) were detected in LG308 treated tumors, while no significant change of angiogenesis indicated by probes anti-CD31 (Supplemental Figure 4A). Thus, LG308 exerted potent antitumor efficacy toward PC-3M tumor xenograft *in vivo*.

LG308 suppresses PC-3M orthotopic tumor growth and metastasis *in vivo*

Next, the impact of LG308 on PC-3M orthotopic tumor growth and metastasis model was evaluated. A luciferase-expressing PC-3M cell line (PC-3M-luc) was constructed

JPET Fast Forward. Published on September 16, 2015 as DOI: 10.1124/jpet.115.225912
This article has not been copyedited and formatted. The final version may differ from this version.

before cells were injected into the dorsal prostate. As Figure 5A shown, at the day the nude mice were sacrificed, the average normalized photon flux of the 10 mg/kg/day of LG308 treated group and 25 mg/kg/day of LG308 treated group was 35.27 ± 18.45 percent and 11.04 ± 9.95 percent of that of control group, respectively. The average tumor volume of control group was 1230.71 ± 663.10 mm^3, while that of 10 and 25 mg/kg/day of LG308 treated group were 388.18 ± 46.98 mm^3 and 209.95 ± 144.47 mm^3, respectively (Fig. 5D). The tumor of control group spread to other organs obviously, like intestine, liver, kidney and spleen. However, LG308 treated group didn't develop obvious metastasis (Fig. 5B). And at the same time, treatment of LG308 with the given concentration had little influence on the body weights of the LG308-treated mice, compared with control group (Fig. 5C). In conclusion, these results indicate that LG308 not only inhibits the growth of PC-3M tumor xenograft, but also hinders PC-3M orthotopic tumor growth and metastasis *in vivo*.

The concentration of LG308 in nude mouse plasma

As shown in Supplemental Figure 4B, the concentration of LG308 in nude mouse plasma at 10 min was 6885.01 ng/mL and 3580.55 ng/mL after intraperitoneal administration of LG308 with the doses at 25 mg/kg and 10 mg/kg, which far exceed its effective concentration *in vitro*. And it could still reach 362.19 ng/mL and 38.25 ng/mL after 8h, respectively. These data could support its pharmacological effects *in vivo*.

Discussion

In the present study, we described a small molecular compound LG308 that inhibits prostatic tumor growth and metastasis. LG308 inhibited the proliferation of androgen dependent (LNCaP, 22RV1) or independent (PC-3M, DU145, PC3) PCa cells *in vitro* and suppressed PC-3M tumor growth and metastasis via blocking the polymerization of microtubule.

In the past few years, great strides have been made for identifying effective and new therapies for PCa (Shore et al., 2012). But most PCa cases ultimately relapsed and progressed to intractable castration-resistant PCa (CRPC)(Xu and Zhang, 2014). Traditional chemotherapy was applied in clinical for the treatment of CRPC. Docetaxel and cabazitaxel are well established anti-microtubule chemotherapy agent with significant survival benefits in CRPC treatment (McKeage, 2012). The successful use of docetaxel and cabazitaxel in PCa chemotherapy suggested that microtubule-targeting agents may be a feasible strategy in treating. However, although they have been extensively used, many problems remains including drug resistance and concomitant side effects (Kavallaris, 2010). So, it is necessary to develop new agents that overcome these hurdles. In our study , we showed that LG308 inhibited the polymerization of tubulin in a concentration-dependent manner. Polymerized tubulin decreased significantly when responding to LG308 exposure in the microtubule polymerization assay in PC-3M and LNCaP cells. We also observed disorganized microtubule distribution in interphase and disrupted spindle in mitotic phase of PC-3M

and LNCaP cells. Moreover the scattered staining increased with the concentration increase of LG308.In accordance with the fact that microtubule-targeting agents arrest the cell cycle at G2/M phase, our results showed that LG308 induced a G2/M blockade, as indicated by flow cytometry analysis (Fig. 1D). We further investigated the in-depth molecular mechanism of cell cycle arrest induced by LG308. Cyclin B and cdc2 kinase regulated the start of M phase (King and Cidlowski, 1995). Previous research have shown that the activation of cdc2 kinase is dependent on accumulation of cyclin B and dephosphorylation of cdc2 (Chiang et al., 2013). We observed an obvious dose-dependent decrease of phosphorylated cdc2 protein and total cdc25c protein in PC-3M and LNCaP, and an accumulation of cyclin B1 protein in PC-3M. Meanwhile, the level of total cdc2 was not affected by the treatment of LG308. Previous studies have shown that MPM2 was a protein related to mitotic (Scatena et al., 1998). And the MPM-2 up-regulation accompanied by the increase of LG308 concentration was detected in our study. Cell cycle arrest at mitotic phase might be an upstream event leading to apoptotic (Jordan and Wilson, 2004). Significant cell apoptosis and cell death induced by LG308 were detected by flow cytometry analysis and cell live/dead assay in PCa cells (Fig. 3A, 3B and 3C). In conclusion, LG308 is a promising anticancer candidate with anti-microtubule activity for the treatment of prostate cancer according to our research.

Besides the primary advantage of LG308 that it possesses remarkable anticancer effectiveness *in vitro* and *in vivo*, another advantage of LG308 is its acceptable toxicity. In fact, drugs possessing anti-microtubule activity have been used in clinic as

anti-cancer drugs for several years (Zhang et al., 2015) but many obstacles to effective treatment with currently approved agents are present, incorporating significant side effects (Risinger et al., 2009b; Novio et al., 2014). According to our research, LG308 has acceptable toxicity. Although LG308 induced cell cycle arrest in PNT1A, a human normal prostate epithelium immortalized cell line, as well as PCa cell lines, and it only shows slight proliferation inhibition in PNT1A cells with the effective concentration in PCa cell lines. LG308 at the effective concentration had little effect on the body weight of the LG308-treated mice *in vivo*, when compared to the control group in subcutaneous xenograft tumor model and orthotopic growth and metastasis model (Fig. 4A and Fig. 5C). There was also no significant difference in HE staining results of liver and kidney between LG308-treated group and control group (Fig. 4C).

Our study had a few limitations. Although LG308 had the inhibitory effect on microtubule polymerization, we still did not know the specific. It was not clear whether LG308 exerted its inhibitive effect on microtubule polymerization by direct combination with tubulin or through some other ways. Meanwhile, apoptosis and cell death induced by anti-mitotic agents were known to be related to alternations of cellular signaling pathways, but the specific mechanism of LG308 in PCa were not clear enough. What's more, we also tested some symbolic parameters of pharmacokinetics and pharmacodynamics (PDPK) about LG308 *in vivo*, more study need to determine more specific PDPK characteristics for its preclinical study in the future.

In conclusion, our data demonstrated LG308, a novel small molecule compound

designed and synthesized, was efficacious in suppressing the growth and metastasis of PCa both *in vitro* and *in vivo* via perturbing the microtubule polymerization primarily. As a result, LG308 can be considered as a new potential drug candidate in for PCa, and it was worth further research and investigation.

JPET Fast Forward. Published on September 16, 2015 as DOI: 10.1124/jpet.115.225912
This article has not been copyedited and formatted. The final version may differ from this version.

Acknowledgments

We thank Dr. Hanyi Zhuang (Shanghai Jiaotong University) for support of cell lines and thank all members of Dr Mingyao Liu' lab in East China Normal University.

JPET Fast Forward. Published on September 16, 2015 as DOI: 10.1124/jpet.115.225912
This article has not been copyedited and formatted. The final version may differ from this version.

Authorship Contributions

Participated in research design: Qin, Peng, Wang, M.Y. Liu, Y.H. Chen and Yi

Conducted experiments: Qin, Peng, Hu, Y.D. He, H. Chen, Y. He, A. Chen, and Yi

Contributed new reagents or analytic tools: N. Liu, Li and Y.H. Chen

Performed data analysis: Qin, Peng, Hu and H. Chen

Wrote or contributed to the writing of the manuscript: Qin, Peng, N. Liu, Hu, Y.D. He, Y. He, A. Chen, Y.H. Chen and Yi

References

Amos LA (2000) Focusing-in on microtubules. *Current opinion in structural biology* **10**:236-241.

Aneja R, Miyagi T, Karna P, Ezell T, Shukla D, Vij Gupta M, Yates C, Chinni SR, Zhau H, Chung LW and Joshi HC A novel microtubule-modulating agent induces mitochondrially driven caspase-dependent apoptosis via mitotic checkpoint activation in human prostate cancer cells. *Eur J Cancer* **46**:1668-1678.

Aneja R, Miyagi T, Karna P, Ezell T, Shukla D, Vij Gupta M, Yates C, Chinni SR, Zhau H, Chung LW and Joshi HC (2010) A novel microtubule-modulating agent induces mitochondrially driven caspase-dependent apoptosis via mitotic checkpoint activation in human prostate cancer cells. *Eur J Cancer* **46**:1668-1678.

Caty A, Oudard S, Humblet Y, Beauduin M, Suc E, Gil T, Rolland F, Houyau P, Sun X, Montcuquet P, Breza J, Favreau E, Tresca P and Chopin D (1997) Phase II study of vinorelbine in patients with hormone refractory prostate cancer. *European Journal of Cancer* **33**:135-135.

Chang CH, Yu FY, Wu TS, Wang LT and Liu BH Mycotoxin citrinin induced cell cycle G2/M arrest and numerical chromosomal aberration associated with disruption of microtubule formation in human cells. *Toxicol Sci* **119**:84-92.

Chang CH, Yu FY, Wu TS, Wang LT and Liu BH (2011) Mycotoxin citrinin induced cell cycle G2/M arrest and numerical chromosomal aberration associated with disruption of microtubule formation in human cells. *Toxicological sciences : an official journal of the Society of Toxicology* **119**:84-92.

Chiang NJ, Lin CI, Liou JP, Kuo CC, Chang CY, Chen LT and Chang JY (2013) A novel synthetic

microtubule inhibitor, MPT0B214 exhibits antitumor activity in human tumor cells through mitochondria-dependent intrinsic pathway. *PloS one* **8**:e58953.

Desbene S and Giorgi-Renault S (2002) Drugs that inhibit tubulin polymerization: the particular case of podophyllotoxin and analogues. *Current medicinal chemistry Anti-cancer agents* **2**:71-90.

Dong Y, Lu B, Zhang X, Zhang J, Lai L, Li D, Wu Y, Song Y, Luo J, Pang X, Yi Z and Liu M (2010) Cucurbitacin E, a tetracyclic triterpenes compound from Chinese medicine, inhibits tumor angiogenesis through VEGFR2-mediated Jak2-STAT3 signaling pathway. *Carcinogenesis* **31**:2097-2104.

Jani AB and Hellman S (2003) Early prostate cancer: clinical decision-making. *Lancet* **361**:1045-1053.

Jordan MA and Wilson L (2004) Microtubules as a target for anticancer drugs. *Nat Rev Cancer* **4**:253-265.

Kavallaris M (2010) Microtubules and resistance to tubulin-binding agents. *Nat Rev Cancer* **10**:194-204.

Kearns B, Lloyd Jones M, Stevenson M and Littlewood C (2013) Cabazitaxel for the second-line treatment of metastatic hormone-refractory prostate cancer: a NICE single technology appraisal. *PharmacoEconomics* **31**:479-488.

King KL and Cidlowski JA (1995) Cell cycle and apoptosis: common pathways to life and death. *Journal of cellular biochemistry* **58**:175-180.

Kuo CC, Hsieh HP, Pan WY, Chen CP, Liou JP, Lee SJ, Chang YL, Chen LT, Chen CT and Chang JY (2004) BPR0L075, a novel synthetic indole compound with antimitotic activity in human cancer cells, exerts effective antitumoral activity in vivo. *Cancer Res* **64**:4621-4628.

McIntosh JR and Hering GE (1991) Spindle fiber action and chromosome movement. *Annual review of cell biology* **7**:403-426.

McKeage K (2012) Docetaxel: a review of its use for the first-line treatment of advanced castration-resistant prostate cancer. *Drugs* **72**:1559-1577.

Miyamoto H, Messing EM and Chang C (2004) Androgen deprivation therapy for prostate cancer: current status and future prospects. *The Prostate* **61**:332-353.

Morganti AG, Massaccesi M, Caravatta L, Macchia G, Picardi V, Deodato F, Ippolito E, Mignogna S, Ferro M, Cilla S, Mattiucci GC and Valentini V (2013) Radiotherapy and Concurrent Metronomic Chemotherapy in Hormone-refractory Prostate Carcinoma: A Phase I Study. *Anticancer Res* **33**:4585-4589.

Novio S, Freire-Garabal M and Nunez MJ (2014) Target driven preclinical screening for new antimitotic chemotherapy agents. *Current topics in medicinal chemistry* **14**:2263-2271.

Pettaway CA, Pathak S, Greene G, Ramirez E, Wilson MR, Killion JJ and Fidler IJ (1996) Selection of highly metastatic variants of different human prostatic carcinomas using orthotopic implantation in nude mice. *Clin Cancer Res* **2**:1627-1636.

Ponholzer A, Steinbacher F, Madersbacher S and Schramek P (2011) [Current treatment of locally advanced and metastatic prostate cancer]. *Wien Med Wochenschr* **161**:377-381.

Ren SC, Chen R and Sun YH (2013) Prostate cancer research in China. *Asian journal of andrology* **15**:350-353.

Risinger AL, Giles FJ and Mooberry SL (2009a) Microtubule dynamics as a target in oncology. *Cancer treatment reviews* **35**:255-261.

Risinger AL, Giles FJ and Mooberry SL (2009b) Microtubule dynamics as a target in oncology. *Cancer treatment reviews* **35**:255-261.

Scatena CD, Stewart ZA, Mays D, Tang LJ, Keefer CJ, Leach SD and Pietenpol JA (1998) Mitotic

phosphorylation of Bcl-2 during normal cell cycle progression and Taxol-induced growth arrest. *The Journal of biological chemistry* **273**:30777-30784.

Shi K, Jiang Q, Li Z, Shan L, Li F, An J, Yang Y and Xu C Sodium selenite alters microtubule assembly and induces apoptosis in vitro and in vivo. *J Hematol Oncol* **6**:7.

Shore N, Mason M and de Reijke TM (2012) New developments in castrate-resistant prostate cancer. *BJU international* **109 Suppl 6**:22-32.

Siegel RL, Miller KD and Jemal A (2015) Cancer statistics, 2015. *CA: a cancer journal for clinicians* **65**:5-29.

Stumpff J, Ghule PN, Shimamura A, Stein JL and Greenblatt M (2014) Spindle microtubule dysfunction and cancer predisposition. *Journal of cellular physiology* **229**:1881-1883.

Suzman DL and Antonarakis ES (2014) Castration-resistant prostate cancer: latest evidence and therapeutic implications. *Therapeutic advances in medical oncology* **6**:167-179.

Tuomela JM, Valta MP, Vaananen K and Harkonen PL (2008) Alendronate decreases orthotopic PC-3 prostate tumor growth and metastasis to prostate-draining lymph nodes in nude mice. *BMC Cancer* **8**:81.

Wilson L and Jordan MA (1995) Microtubule dynamics: taking aim at a moving target. *Chemistry & biology* **2**:569-573.

Xu S and Zhang ZY (2014) [Updated treatment of castration-resistant prostate cancer]. *Zhonghua nan ke xue = National journal of andrology* **20**:1136-1140.

Zhang CC, Yan Z, Zhang Q, Kuszpit K, Zasadny K, Qiu M, Painter CL, Wong A, Kraynov E, Arango ME, Mehta PP, Popoff I, Casperson GF, Los G, Bender S, Anderes K, Christensen JG and VanArsdale T PF-03732010: a fully human monoclonal antibody against P-cadherin with

antitumor and antimetastatic activity. *Clin Cancer Res* **16**:5177-5188.

Zhang H, Wang C, Jiang T, Guo H, Wang G, Cai X, Yang L, Zhang Y, Yu H, Wang H and Jiang K (2015) Microtubule-targetable fluorescent probe: site-specific detection and super-resolution imaging of ultratrace tubulin in microtubules of living cancer cells. *Analytical chemistry* **87**:5216-5222.

Zhang T, Li J, Dong Y, Zhai D, Lai L, Dai F, Deng H, Chen Y, Liu M and Yi Z (2012) Cucurbitacin E inhibits breast tumor metastasis by suppressing cell migration and invasion. *Breast cancer research and treatment* **135**:445-458.

Zhang XL, Song YJ, Wu YY, Dong YM, Lai L, Zhang J, Lu BB, Dai FJ, He LJ, Liu MY and Yi ZF (2011) Indirubin inhibits tumor growth by antitumor angiogenesis via blocking VEGFR2-mediated JAK/STAT3 signaling in endothelial cell. *Int J Cancer* **129**:2502-2511.

Zhao H, Quan H, Xie C, Xu Y, Xie F, Hu Y and Lou L YHHU0895, a novel synthetic small-molecule microtubule-destabilizing agent, effectively overcomes P-glycoprotein-mediated tumor multidrug resistance. *Cancer Lett* **314**:54-62.

JPET Fast Forward. Published on September 16, 2015 as DOI: 10.1124/jpet.115.225912
This article has not been copyedited and formatted. The final version may differ from this version.

Footnotes

This work was supported by Major State Basic Research Development Program of China [Grants 2015CB910400, 2012CB910400]; National Natural Science Foundation of China [Grants 81272463, 81472788, 81330049, 81202407]; and Innovation Program of Shanghai Municipal Education Commission [Grant 13zz034].

Zhengfang Yi, Shanghai Key Laboratory of Regulatory Biology, Institute of Biomedical Sciences and School of Life Sciences, East China Normal University, 500 Dongchuan Rd, Shanghai, 200241, China; zfyi@bio.ecnu.edu.cn

[1]Min Qin, [2]Shihong Peng, [3]Ning Liu, [4]Meichun Hu, [5]Yundong He, [6]Guoliang Li, [7]Huang Chen, [8]Yuan He, [9]Ang Chen, [10]Xin Wang, [11]Mingyao Liu, [12]Yihua Chen and [13]Zhengfang Yi

M.Q. and S.P. contributed equally to this work.

JPET Fast Forward. Published on September 16, 2015 as DOI: 10.1124/jpet.115.225912
This article has not been copyedited and formatted. The final version may differ from this version.

Figure Legends

Fig. 1. A, chemical structure, molecular formula and 308.3495 molecular weight of LG308. B, LG308 more potently inhibited the proliferation of several PCa cells than normal prostate epithelium cells. Cells were incubated with different dose of LG308 for 72 h in 96-well plates and the cell viability was tested by SRB assay. n=3; **, P<0.01; ***, P<0.001. C, LG308 inhibited colony formation of PCa cells PC-3M and LNCaP. After treatment by different doses of LG308 in 6-well plates for a week, cells were fixed and stained with crystal violet and the numbers of cell colonies were counted. n=3; ***, P<0.001. D, LG308 induced cell cycle arrest of LNCaP and PC-3M cell lines. Cells were analyzed by flow cytometry after treatment of LG308 with different doses for 24 h. E, Effect of LG308 on the expression of G2/M transition related proteins. After incubation with different doses of LG308 for 24 h, cells were lysed and cdc2, p-cdc2, cdc25c, cyclin B1 and β-actin were measured by western blotting analysis with their specific antibodies.

Fig. 2. A, LG308 increased accumulation of mitotic PC-3M cells. PC-3M cells were exposed to different dose of LG308 for 24h. Total and mitosis phase cells were counted. The mitotic index was represented by percentage of mitosis phase cells. Red arrows point to mitotic cells. n=3; **, P<0.01; ***, P<0.001. B, LG308 increased expression of MPM-2 in PC-3M cells. PC-3M cells were treated with different dose of LG308 for 24 h and MPM-2 was measured by western blotting analysis with

specific antibody. C, LG308 reduced polymerized tubulin in PC-3M and LNCaP cells. Cells were treated with different doses of LG308 or 50 nM colchicine (served as positive control) or 50 nM paclitaxel (served as negative control) for 24 h. Then separated polymerized tubulin and total tubulin were detected by western blotting analysis with tubulin antibodies. D and E, LG308 disrupted the microtubule organization in interphase and mitotic phase in PC-3M cells. PC-3M cells were treated with different dose of LG308 or 50 nM colchicine (served as positive control) or 50 nM paclitaxel (served as negative control) for 24h. Cells were fixed and the network of microtubulin was stained with α-tubulin antibody (green) and the nuclear DNA was stained by DAPI (blue). Images of interphase cells (D) and mitotic phase cells (E) were taken by confocal microscopy. Red arrows point to microtubulin.

Fig. 3. A and B, LG308 mediated PC-3M cells apoptosis in dose-dependent and time-dependent manner. Cells were treated with different dose of LG308 for 48 h (A) or with 10 μM LG308 for 24 h, 48 h, and 72 h (B). Then the percentage of apoptosis cells was analyzed with flow cytometry. C, LG308 destroyed plasma membrane integrity of PC-3M and LNCaP cells. PC-3M cells were treated with different dose of LG308 for 48 h and stained by live-dead kit. Representative image at 10 μM was showed. The red represented dead cells while the green represented live cells. Red arrows point to dead cells. Quantitative data of different does was showed on the right. n=3; ***, $P<0.001$.

JPET Fast Forward. Published on September 16, 2015 as DOI: 10.1124/jpet.115.225912
This article has not been copyedited and formatted. The final version may differ from this version.

Fig. 4. A, PC-3M tumor-bearing mice were intraperitoneally treated with LG308 (25 mg/kg/day) or DMSO (served as control) for 20 days. Tumor volume and mice body weight were measured 3 times a week during LG308 administration and weight of removed tumor was also measured. n=8; ns, no significant; *, P<0.05; ***, P<0.001. B, Expression of Ki-67 decreased while MPM-2 increased in LG308-treatment group. For Ki-67 and MPM-2 immunohistochemical staining, sections which cut from the paraffin blocks of PC-3M xenograft were carried out using Ki-67 or MPM-2 antibody and the positive cells (brown color) of each group were counted. n=3; ***, P<0.001. C, Liver and kidney hematoxylin and eosin (HE) staining of control and LG308-treatment group.

Fig. 5. A and B, PC-3M-luc tumors were imaged by IVIS and tumor volume was represented by the normalized photon flux and separated tumors, metastasis and organs were also imaged by IVIS. n=8; **, P<0.01. C, Mice body weight was measured every 2 days during LG308 treatment. ns, no significant. D, Orthotopic tumors were removed and images were taken and volume of tumors was measured. n=8; **, P<0.01.

JPET Fast Forward. Published on September 16, 2015 as DOI: 10.1124/jpet.115.225912

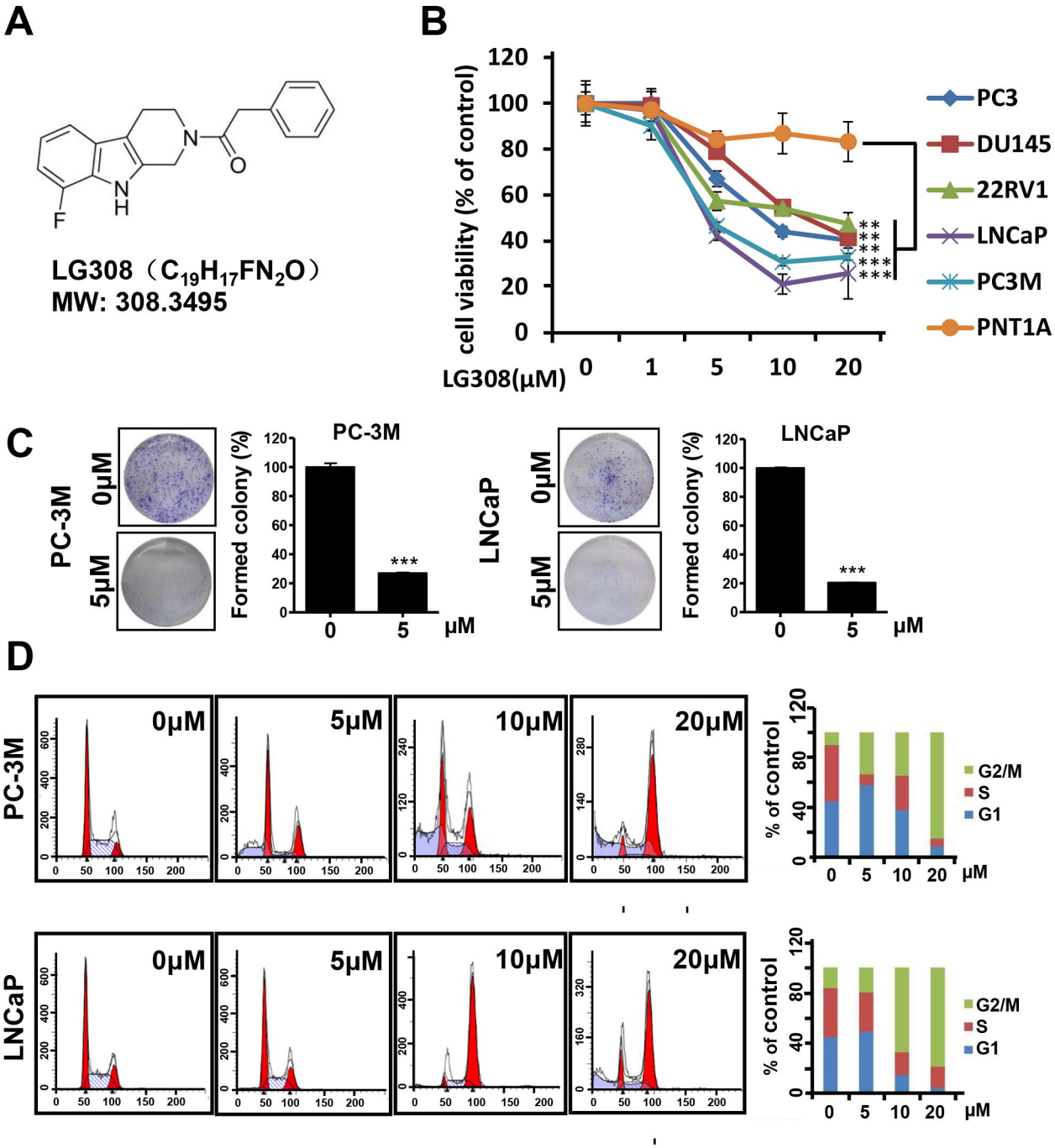

Figure 1

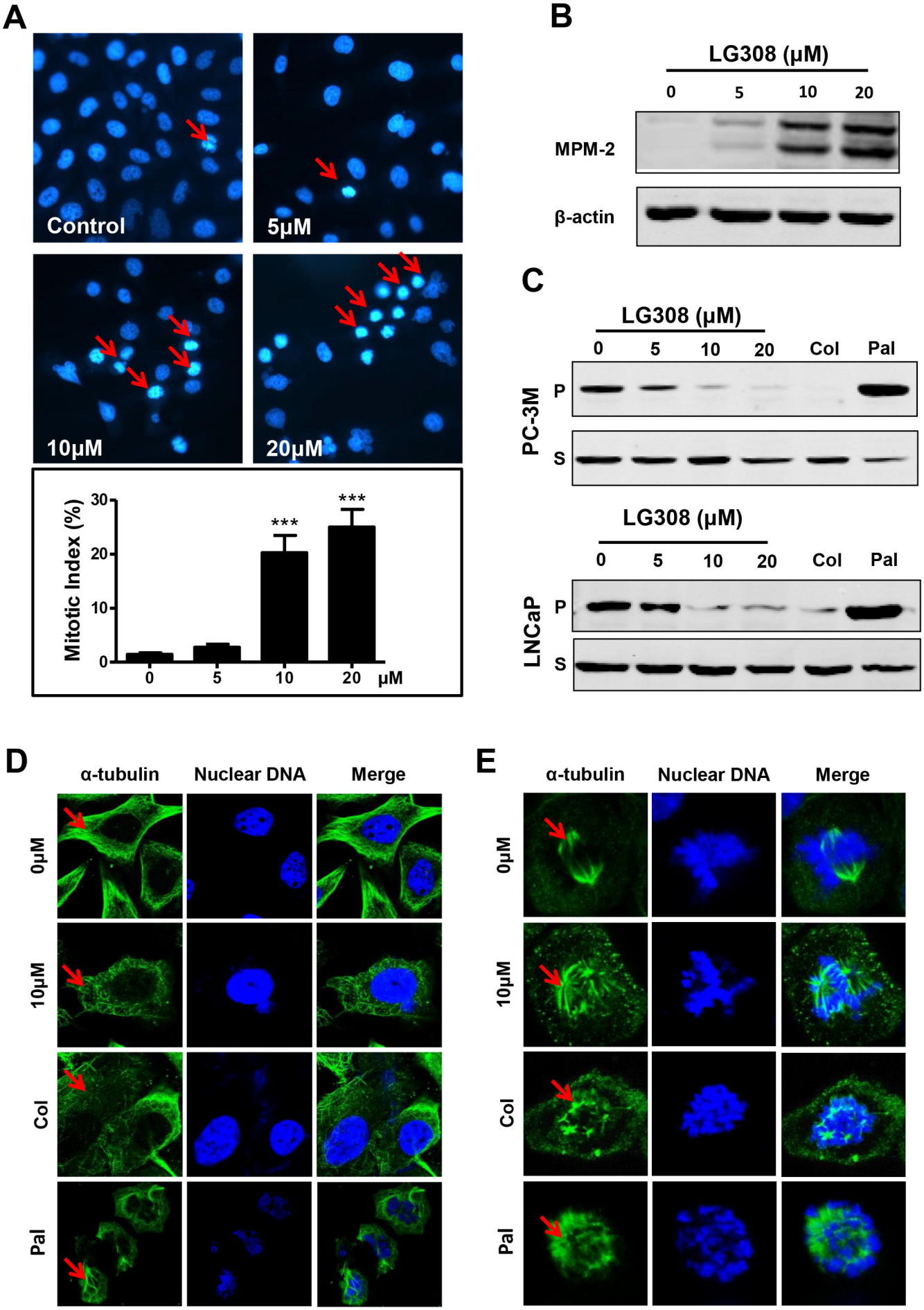

Figure 2

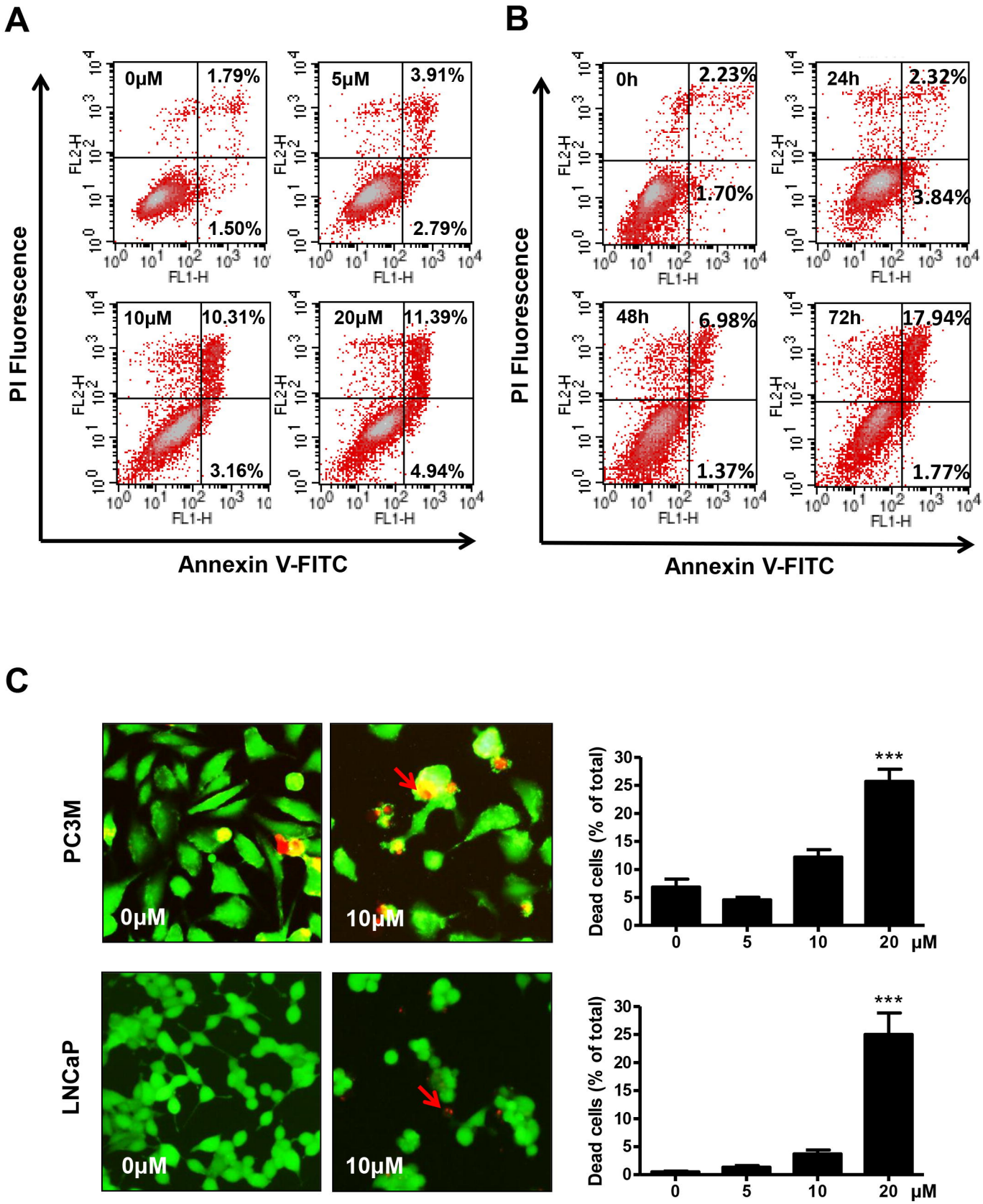
A
0μM
1.79%
1.50%
5μM
3.91%
2.79%
10μM
10.31%
3.16%
20μM
11.39%
4.94%
PI Fluorescence
Annexin V-FITC
FL2-H
FL1-H
B
0h
2.23%
1.70%
24h
2.32%
3.84%
48h
6.98%
1.37%
72h
17.94%
1.77%
C
PC3M
LNCaP
0μM
10μM
Dead cells (% of total)
***
0
5
10
20
μM

Figure 3

JPET Fast Forward. Published on September 16, 2015 as DOI: 10.1124/jpet.115.225912

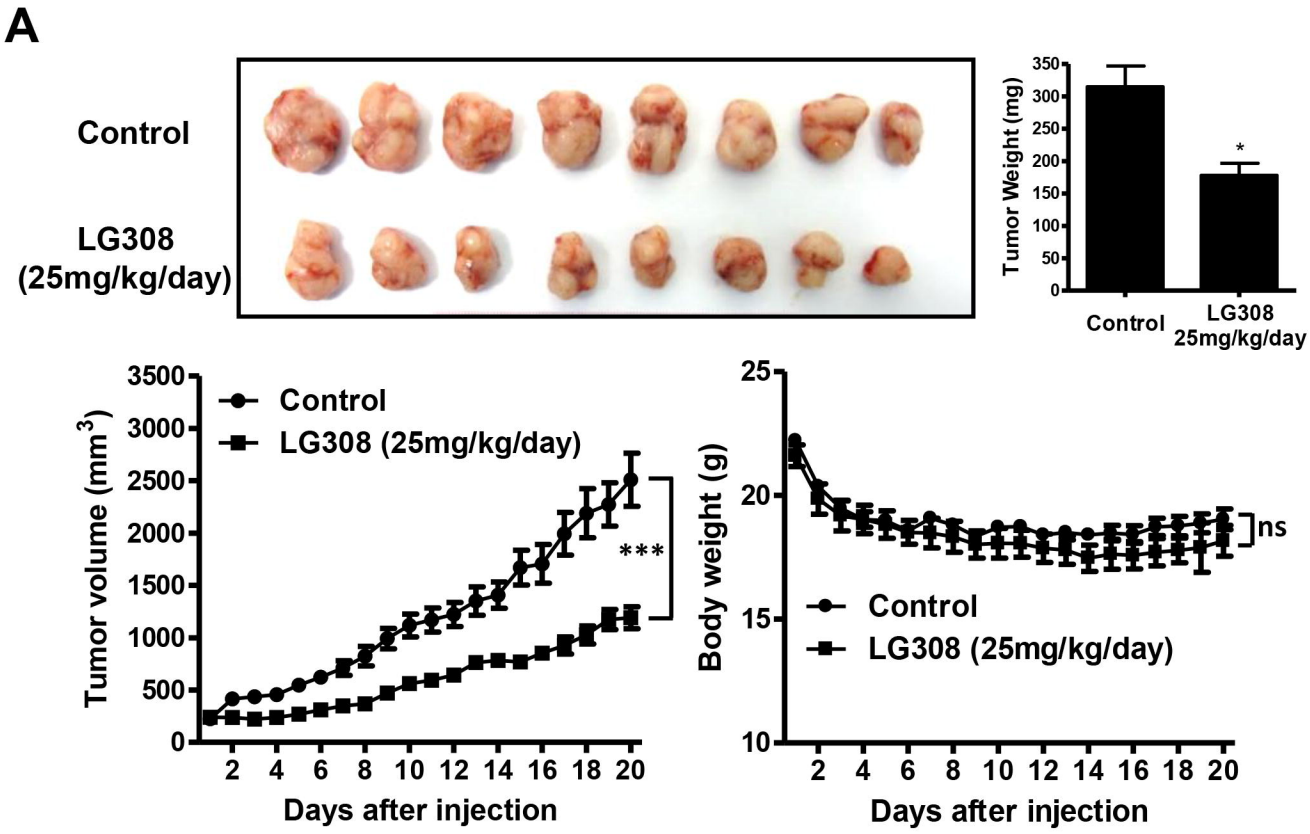

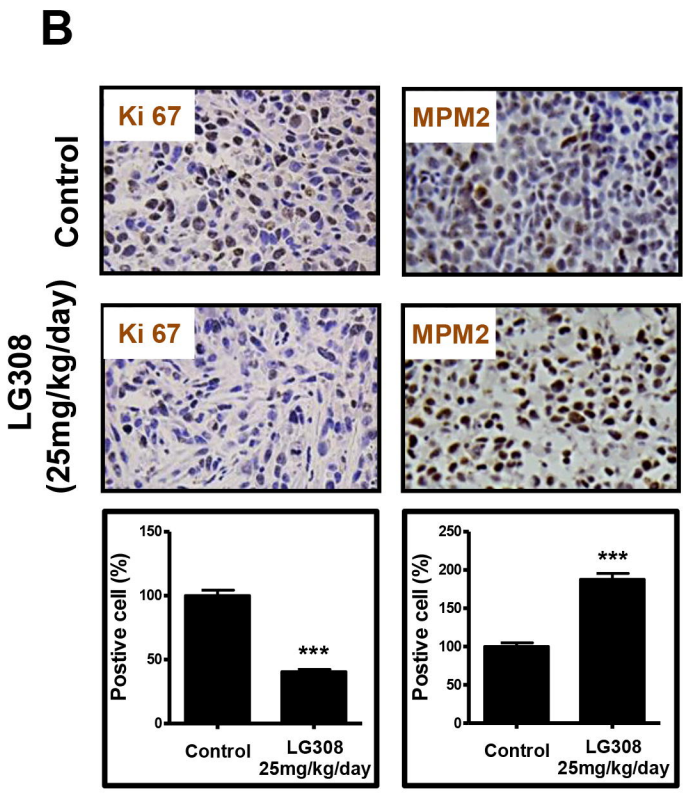

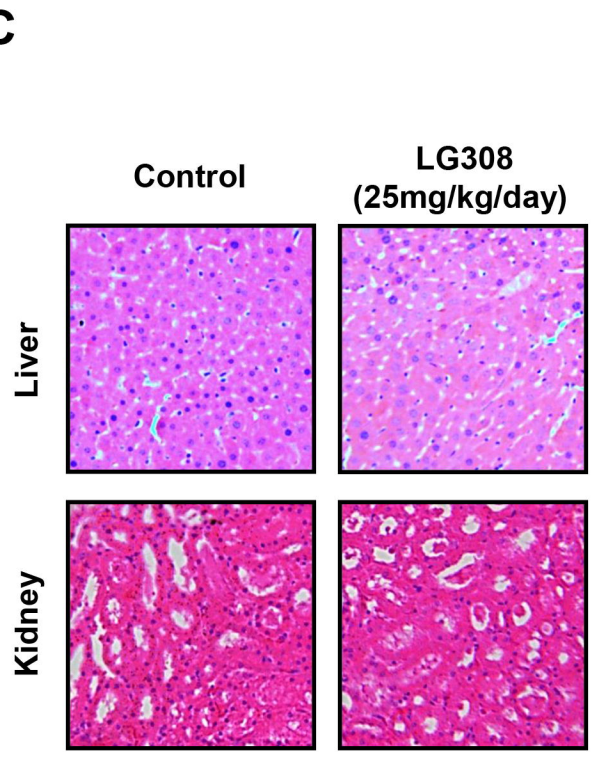

Figure 4

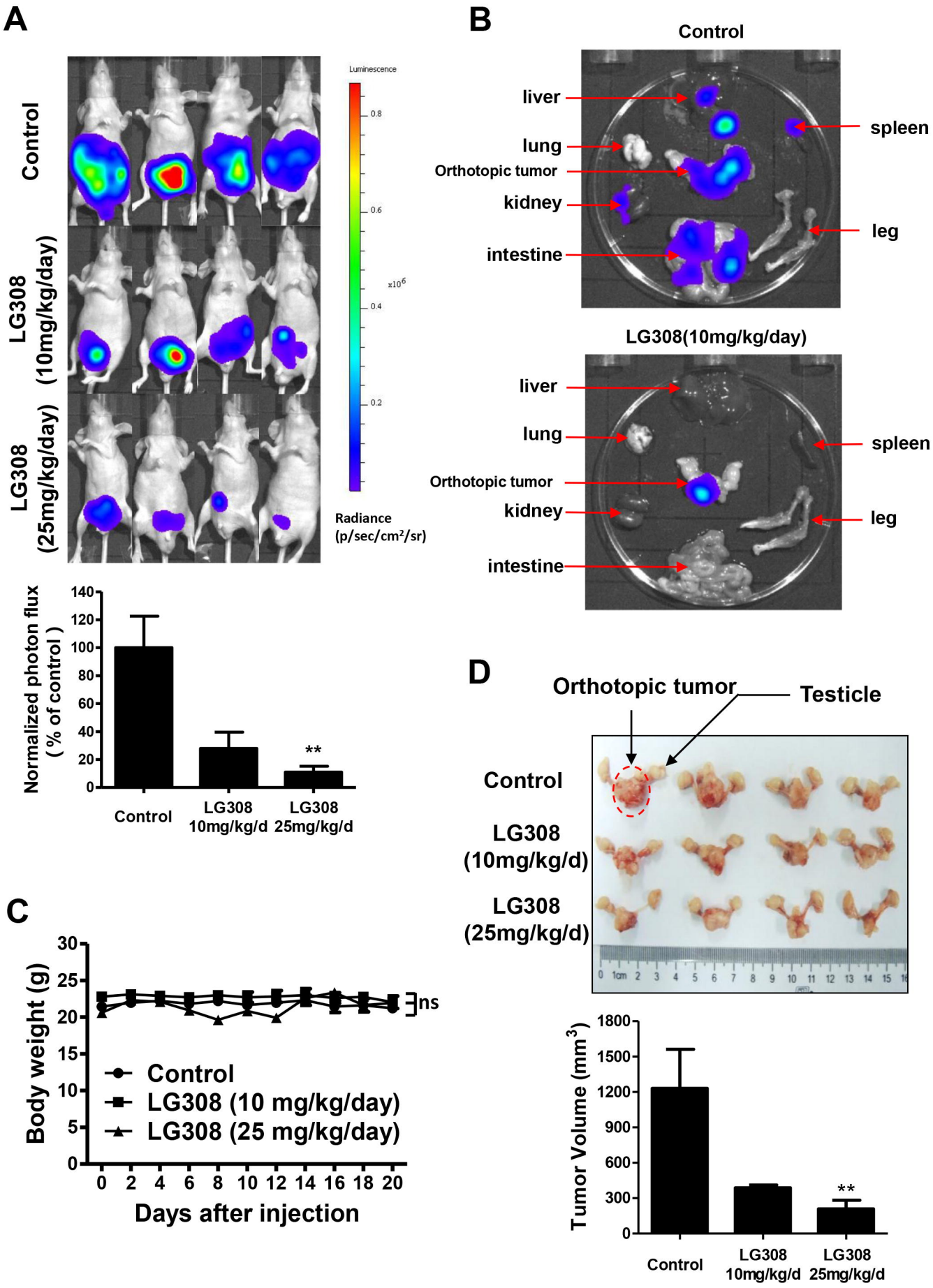

Figure 5